GEOMETRIC ALIGNMENT OF TWO OVERLAPPING RANGE IMAGES

Marcos A Rodrigues, Yonghuai Liu, and *Qian Wei*

School of Computing, Sheffield Hallam University, Sheffield S1 1WB, UK
E-mail {*M.Rodrigues, Y.Liu, Q.Wei*}@shu.ac.uk

ABSTRACT

In this paper, we propose a novel geometric method for the alignment of two overlapping range images. The method first employs the traditional ICP criterion to establish a set of possible correspondences and then refine these correspondences using geometric constraints derived from properties of reflected correspondence vectors. In this way, the method overcomes a major limitation of the traditional ICP criterion which is the introduction of false matches in almost every iteration of the alignment. For an accurate estimation of the geometric parameters of interest, the Monte Carlo method is used in conjunction with a median filter. Finally, the quaternion method is used to estimate the motion parameters based on the refined correspondences. Experimental results based on both synthetic data and real images show that the proposed method can effectively align two overlapping range images with a small motion.

1. INTRODUCTION

With recent technological developments in optics and electronics, range image acquisition systems are becoming more affordable and accurate. Since range images provide depth information, their analysis has proved simpler than that of the model based or projective images, leading to greater potential for applications in a number of tasks such as computer aided geometric design (CAGD), motion analysis, object recognition [5], and reverse engineering [3]. However, the alignment of two overlapping range images is still a fundamental problem in range image analysis. As a result, a large number of techniques have been proposed to deal with this limitation, such as techniques based on iterative closest point algorithm (ICP) [1, 10], interactive method [8], and triangle matching [7], among many others.

The ICP method is the most promising of the image registration methods. Its concept is simple and relatively easy to implement. However, the problem of the ICP algorithm is that the criterion used to establish correspondences often unavoidably introduces false matches in almost every iteration of the alignment since it just uses the distance constraint to determine the position of the correspondents in two range images, when it is known that a position in 3D space can only be uniquely determined by three constraints. Advances have been made through a number of proposed techniques to improve the ICP method such as spin images [5], bitangent curves [9], and normal and tangent information [4]. A careful analysis reveals that these methods either employ invariants described in a single coordinate to reduce false matches, or use thresholds or perform the general χ^2 test to reject false matches. The problem still remains because invariants cannot theoretically completely eliminate false matches, thresholds are context dependent and often are not easily determined, and the χ^2 test depends on the estimation of the uncertainty of every point.

In this paper, we propose a novel geometric method for the alignment of two overlapping range images representing a significant improvement to the traditional ICP method. This novel method first employs the ICP criterion [1] to establish a set of possible correspondences between the two range images to be aligned. Since false matches are created by the motion, we argue that their elimination can only be carried out using the properties of the motion. In [6], we extended Chasles' screw motion theory by analysing the geometric properties of reflected correspondence vectors synthesised into a single coordinate frame. Such analysis has provided an exact insight into the physical interpretation of rigid motion constraints bridging the points described in different coordinate frames before and after a motion. Thus, the novel method then employs the geometric properties of reflected correspondence vectors to evaluate whether possible correspondences are plausible or not yielding a set of refined correspondences. In order to improve the accuracy and efficiency of the geometric parameter estimation, the Monte Carlo method in conjunction with a median filter are employed. Finally, this novel method employs the quaternion method [1] to estimate the motion parameters based on the refined correspondences. The proposed alignment model has been validated through experiments based on both synthetic data and real images. Experimental results have shown that the proposed algorithm is accurate and robust for the alignment of two overlapping range images with a small motion.

The rest of this paper is organised as follows. Section 2

outlines the geometric properties of reflected correspondence vectors as described in [6]. Section 3 describes the proposed algorithm. Section 4 presents experimental results and finally, some conclusions are drawn in Section 5.

2. OUTLINE OF GEOMETRIC PROPERTIES OF REFLECTED CORRESPONDENCE VECTORS

In this section, the geometric properties of reflected correspondence vectors as presented in [6] are outlined with the purpose of formalising additional constraints for false match elimination. A rigid motion can be represented by the following relationship:

$$\mathbf{p}' = \mathbf{R}\mathbf{p} + \mathbf{t} \tag{1}$$

where $\mathbf{R}$ and $\mathbf{t}$ are the rigid rotation matrix and translation vector. The point pair $(\mathbf{p}, \mathbf{p}')$ represents a correspondence where $\mathbf{p}$ is a point described in one coordinate frame before a motion and $\mathbf{p}'$ is its corresponding point described in another coordinate frame after a motion. The reflected correspondence (**RC**) of $(\mathbf{p}, \mathbf{p}')$ is defined as: $(\mathbf{p}, \mathbf{p}'') = (\mathbf{p}, -\mathbf{p}')$.

Given two sets of correspondence data $(\mathbf{p}_i, \mathbf{p}_i')$ where $i = 1, 2, \cdots, n \mid n \geq 3$, the geometrical properties of reflected correspondence vectors: $\mathbf{RCV}_i = \mathbf{p}_i - \mathbf{p}_i''$ which have been synthesised into a single coordinate frame were analysed and assuming that the rotation angle θ is defined as: $\theta \in [0, \pi)$, the following theorem has been put forward in [6]:

Theorem 1 *A motion $(\mathbf{R}, \mathbf{t})$ is a 3D rigid motion if and only if there exists a fixed axis $\mathbf{h} = (h_x, h_y, h_z)^T$ and a fixed point $\mathbf{e}$, such that:*

$$||\underline{\mathbf{p}} - \underline{\mathbf{e}}|| = ||\underline{\mathbf{p}}'' - \underline{\mathbf{e}}|| \tag{2}$$

$$\frac{(\underline{\mathbf{p}} - \underline{\mathbf{e}})^T(\underline{\mathbf{p}}'' - \underline{\mathbf{e}})}{(\underline{\mathbf{p}} - \underline{\mathbf{e}})^T(\underline{\mathbf{p}} - \underline{\mathbf{e}})} = \cos(\pi - \theta) \tag{3}$$

$$\mathbf{h}^T(\mathbf{p} + \mathbf{p}'') = 2\mathbf{h}^T\mathbf{e} \tag{4}$$

where $\cos(\pi - \theta)$ is constant uniquely determined by the rigid motion and $(\underline{\mathbf{p}}, \underline{\mathbf{p}}'')$ is the projection of an arbitrary $\mathbf{RC}$ $(\mathbf{p}, \mathbf{p}'')$ in the plane perpendicular to $\mathbf{h}$.

The fixed axis $\mathbf{h}$ and the fixed point $\mathbf{e}$ in this theorem are called the rotation axis and the essential point respectively. This theorem provides an exact insight into the physical interpretation of rigid motion constraints about distance, angle, and projection information. It says that once a set of points undergo a rigid motion, then their corresponding $\mathbf{RC}$s must satisfy the constraints represented by Equations 2, 3, and 4. If a pair of points do not satisfy any constraint represented by one of Equations 2, 3, and 4, then they cannot represent a $\mathbf{RC}$. From this theorem, we have the following corollary:

Corollary 1 *Both an arbitrary $\mathbf{RC}$ $(\mathbf{p}, \mathbf{p}'')$ and its projection $(\underline{\mathbf{p}}, \underline{\mathbf{p}}'')$ in the plane perpendicular to the rotation axis $\mathbf{h}$ are equidistant to the essential point $\mathbf{e}$:*

$$||\mathbf{p} - \mathbf{e}|| = ||\mathbf{p}'' - \mathbf{e}|| \tag{5}$$

$$||\underline{\mathbf{p}} - \mathbf{e}|| = ||\underline{\mathbf{p}}'' - \mathbf{e}|| \tag{6}$$

Thus, the theorem and its resulting corollary have provided a number of useful rigid motion constraints bridging the points described in different coordinate frames before and after a rigid motion. These constraints can be used to evaluate whether a point pair is really a correspondence or not without a complete calibration of motion parameters as described below.

3. THE NOVEL RCV-ICP ALGORITHM

In this Section a novel method to align two overlapping range images is presented. The method is based on relative gap constraints derived from the above geometric properties. The algorithm is called geometric ICP algorithm based on reflected correspondence vectors (RCV-ICP). First, the ICP criterion is used to find a set of possible correspondences $\mathbf{p}_i'$ $(i = 1, 2, \cdots, n_1)$ for a set of transformed points $\mathbf{p}_i$ $(i = 1, 2, \cdots, n_1)$. Motion properties represented by the essential point $\mathbf{e}$ and the rotation axis $\mathbf{h}$ are then estimated such that relative gaps relative to each possible correspondence can be computed. The essential point $\mathbf{e}$ and the rotation axis $\mathbf{h}$ whose direction is not important here can be estimated by Equations 5 and 4, respectively, as:

$$\begin{pmatrix} \mathbf{RCV}_1^T \\ \mathbf{RCV}_2^T \\ \mathbf{RCV}_3^T \end{pmatrix} \mathbf{e} = \begin{pmatrix} \frac{\mathbf{p}_1^T\mathbf{p}_1 - \mathbf{p}_1''^T\mathbf{p}_1'}{2} \\ \frac{\mathbf{p}_2^T\mathbf{p}_2 - \mathbf{p}_2''^T\mathbf{p}_2'}{2} \\ \frac{\mathbf{p}_3^T\mathbf{p}_3 - \mathbf{p}_3''^T\mathbf{p}_3'}{2} \end{pmatrix} \tag{7}$$

$$\begin{pmatrix} (\mathbf{p}_1 + \mathbf{p}_1'')^T \\ (\mathbf{p}_2 + \mathbf{p}_2'')^T \\ (\mathbf{p}_3 + \mathbf{p}_3'')^T \end{pmatrix} \mathbf{h} = \begin{pmatrix} 1 \\ 1 \\ 1 \end{pmatrix} \tag{8}$$

where $(\mathbf{p}_i, \mathbf{p}_i'')$ $(i = 1, 2, 3)$ are three arbitrary possible $\mathbf{RC}$s. Equations 7 and 8 are linear equation groups which can be robustly solved using the total least squares method [2].

For a more accurate and efficient estimation of the rotation axis $\mathbf{h}$ and the essential point $\mathbf{e}$, the Monte Carlo method is employed. Assuming that a subsample contains m $(m \geq 3)$ correspondences, the whole set of image data are corrupted by false matches with probability ϵ, and the expected probability to obtain an accurate solution is P, then the number N $(N \geq 1)$ of required subsamples can be estimated as:

$$N = \frac{\log(1 - P)}{\log(1 - (1 - \epsilon)^m)} + 1$$

In the experiments described below, the following values were used: let $m = 4$, $\epsilon = 0.7$, and $P = 0.99$, then

$N = 567$. For each subsample, Equations 8 and 7 are used to estimate a candidate to $\mathbf{h}_j$ and $\mathbf{e}_j$ respectively where $j = 1, 2, \cdots, N$. The calibrated rotation axis $\hat{\mathbf{h}}$ and essential point $\hat{\mathbf{e}}$ are estimated by median filtering the corresponding components of $\mathbf{h}_j$ and $\mathbf{e}_j$. False matches are then eliminated as follows:

1. Use Equations 6 and 2 to compute the relative gaps $g1$ and $g2$ relative to each possible $\mathbf{RC}$:

$$g1_i = \frac{|\,||\underline{\mathbf{p}_i} - \hat{\mathbf{e}}|| - ||\underline{\mathbf{p}_i''} - \hat{\mathbf{e}}||\,|}{\max(||\underline{\mathbf{p}_i} - \hat{\mathbf{e}}||, ||\underline{\mathbf{p}_i''} - \hat{\mathbf{e}}||)}$$

$$g2_i = \frac{|\,||\underline{\mathbf{p}_i} - \underline{\hat{\mathbf{e}}}|| - ||\underline{\mathbf{p}_i''} - \underline{\hat{\mathbf{e}}}||\,|}{\max(||\underline{\mathbf{p}_i} - \underline{\hat{\mathbf{e}}}||, ||\underline{\mathbf{p}_i''} - \underline{\hat{\mathbf{e}}}||)}$$

where $\underline{\mathbf{p}_i} = (\mathbf{I} - \hat{\mathbf{h}}\hat{\mathbf{h}}^T)\mathbf{p}_i$, $\underline{\mathbf{p}_i''} = (\mathbf{I} - \hat{\mathbf{h}}\hat{\mathbf{h}}^T)\mathbf{p}_i''$, and $\underline{\hat{\mathbf{e}}} = (\mathbf{I} - \hat{\mathbf{h}}\hat{\mathbf{h}}^T)\hat{\mathbf{e}}$.

2. Compute the mean μ and standard deviation σ of the gaps $g1$ and $g2$:

$$\mu_{g1} = \frac{1}{n_1}\sum_{i=1}^{n_1} g1_i, \;\; \sigma_{g1} = \sqrt{\frac{1}{n_1}\sum_{k=1}^{n_1}(g1_i - \mu_{g1})^2}$$

$$\mu_{g2} = \frac{1}{n_1}\sum_{i=1}^{n_1} g2_i, \;\; \sigma_{g2} = \sqrt{\frac{1}{n_1}\sum_{i=1}^{n_1}(g2_i - \mu_{g2})^2}$$

3. Eliminate false matches: If $|g1_i - \mu_{g1}| > \kappa\ \sigma_{g1}$ or $|g2_i - \mu_{g2}| > \kappa\ \sigma_{g2}$, then the possible correspondence $(\mathbf{p}_i, \mathbf{p}_i')$ is regarded as a false match.

As a result of this procedure, a set of refined correspondences is obtained. Finally, we adopted the quaternion method as described in [1] for motion calibration based on the refined correspondences. The above procedure can be iterated and the criterion as described in [10] was adopted for the algorithm to terminate.

4. EXPERIMENTAL RESULTS

We applied the RCV-ICP algorithm to the image data $\mathbf{P}$ and $\mathbf{P}'$ with the following initial values: $\mathbf{q}^{(0)} = (\sqrt{99}/10, 0.1, 0, 0)^T$, $\mathbf{t}^{(0)} = \bar{\mathbf{p}}' - \bar{\mathbf{p}}$, $\kappa = 1.5$, and maximum iteration number $M = 40$ where $\bar{\mathbf{p}}$ and $\bar{\mathbf{p}}'$ are the centroids of the point sets $\mathbf{P}$ and $\mathbf{P}'$. The experiments are based on both synthetic and real image data.

First, 75 correspondences were created based on a parametric curve [10]. Then zero mean Gaussian noise with standard deviation $\sigma_1 = 0.03$ was added to each coordinate of these correspondences in one series of experiments and $\sigma_2 = 0.06$ in another. Then two sets of image data with appearing and disappearing points were set as $\mathbf{P} = \{\mathbf{p}_1, \mathbf{p}_2, \cdots, \mathbf{p}_{70}\}$ and $\mathbf{P}' = \{\mathbf{p}_6', \mathbf{p}_7', \cdots, \mathbf{p}_{75}'\}$. The experimental results are presented in Figure 1 and Table 1.

Table 1. The average m and standard deviation σ of relative calibration errors in percentage of rotation axis $\hat{\mathbf{h}}$, rotation angle $\hat{\theta}$, and translation vector $\hat{\mathbf{t}}$ and the number k of iterations using synthetic points data.

Noise	Error	$\hat{\mathbf{h}}(\%)$	$\hat{\theta}(\%)$	$\hat{\mathbf{t}}(\%)$	k
σ_1	m	0.062	0.011	0.050	7.643
	σ	0.045	0.005	0.001	1.630
σ_2	m	0.128	0.022	0.101	7.286
	σ	0.088	0.009	0.003	1.385

Table 2. The calibrated rotation matrix $\hat{\mathbf{R}}$, rotation axis $\hat{\mathbf{h}}$, rotation angle $\hat{\theta}$, and translation vector $\hat{\mathbf{t}}$ using bunny range images.

$\hat{\mathbf{R}}$			$\hat{\mathbf{h}}$	θ	$\hat{\mathbf{t}}$
0.951	-0.153	0.269	-0.006		179.314
0.153	0.988	0.019	-0.869	18.021	13.478
-0.269	0.023	0.963	-0.494		-25.775

The bunny range images (Figure 2) used in this paper were downloaded from a publicly available range image database currently hosted by the Signal Analysis and Machine Perception Laboratory at Ohio State University. The sizes of the first and second images were 200×200 and 200×200 which include 6870 and 6874 points, respectively. The images were directly used for experiments without any feature extraction and pre-processing and any knowledge about the distribution of points, occlusion, appearance and disappearance of points, and motion information. The experimental results are presented in Figure 3 and Table 2. The algorithm converges at iteration 17, with average alignment error of 0.515593 and standard deviation of 0.567644. Of 6870 points, the algorithm finds 5964 correspondences in the second image. The time for alignment is 160.0 seconds on a Pentium III, 500MHz, 128MB RAM, 4GB HD computer.

For a clearer visualisation, 200 points were randomly selected with uniform distribution within the first image to show the evolution of alignment as depicted in Figure 3. At iteration 1, these 200 points before and after a rigid motion are relatively far apart in 3D space. But after alignment, 171 of them approximately superimpose with average alignment error of 0.499636 and standard deviation of 0.476130.

An overall analysis of the experiments reveals that the RCV-ICP algorithm is accurate, robust and efficient. The experiments also show that the parameter κ, the distribution of points, and the percentage of appearing and disappearing points included in the image data generally play a vital role in accurate image alignment.

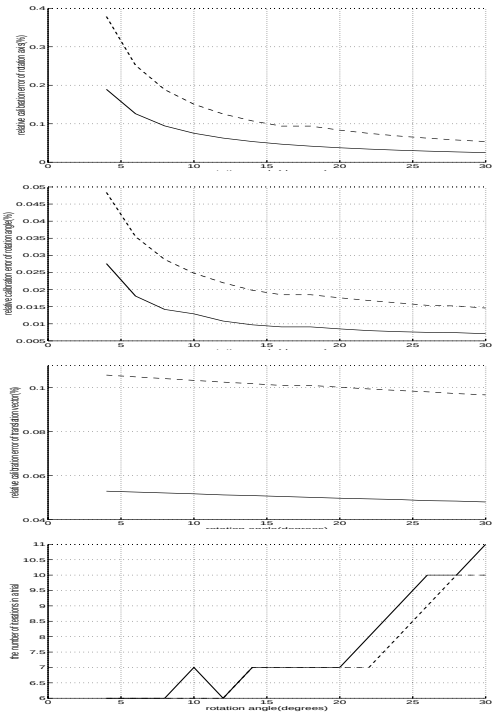

Fig. 1. The plots show calibration errors in percentage for various rotation angles on the horizontal axis against on the vertical axis: the rotation axis (top row), rotation angle (second), translation vector (third), and the number of required iterations (bottom).

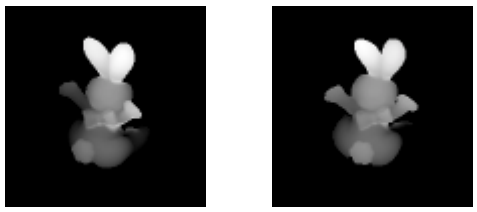

Fig. 2. Two bunny range images from different viewpoints.

5. SUMMARY AND CONCLUSIONS

In this paper, a novel method for aligning two overlapping range images has been presented. Comparing the RCV-ICP algorithm with that described in [1], it has been shown that RCV-ICP can deal with occlusion, appearance and disappearance of points. Comparing the RCV-ICP algorithm with that described in [10], it has been shown that RCV-ICP does not require the user to initialise the maximum tolerance for distance. Thus, it has been demonstrated by a number of experiments based on both synthetic data and real images that the RCV-ICP algorithm is accurate, robust, and efficient for the alignment of two overlapping range images with small motions. Further work involves the investigation of accurate estimation of the parameters of interest from highly corrupted data by outliers. Research is under way and results will be reported in the future.

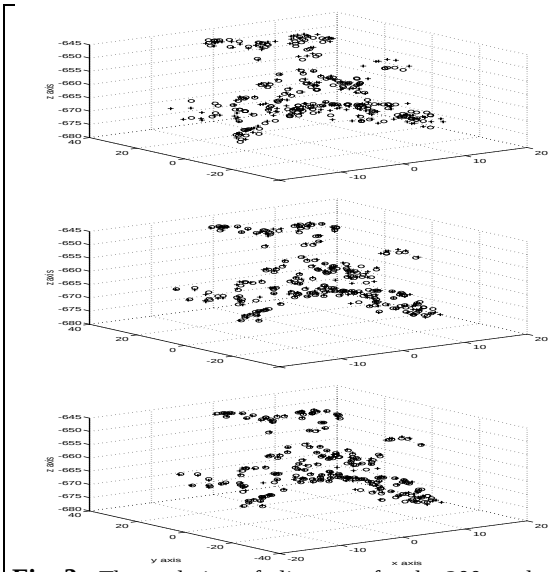

Fig. 3. The evolution of alignment for the 200 randomly selected points with uniform distribution from the first image. Top: alignment at iteration 1; middle: alignment at iteration 8; bottom: after alignment.

6. REFERENCES

[1] P. J. Besl and N. D. McKay. A method for registration of 3D shapes. *IEEE Trans. PAMI*, 14 (1992): 239-256.

[2] G. H. Golub and C. F. Van Loan. *Matrix Computations: the third edition*. The John Hopkins University Press, 1996.

[3] D. W. Eggert et al. Simultaneous registration of multiple range images for use in reverse engineering of CAD models. *CVIU*, 69(1998): 253-272.

[4] J. Feldmar, et al. 3D-2D projective registration of free-form curves and surfaces. *CVIU*, 65(1997): 403-424.

[5] A. Johnson and M. Hebert. Object recognition by matching oriented points. *Proc. IEEE CVPR*, 1997.

[6] Y. Liu and M. A Rodrigues. Essential representation and calibration of rigid body transformations. *Machine Graphics and Vision*, 2000, 9(1/2): 123-138.

[7] G. Roth. Registering two overlapping range images. *Proc. 1997 Int. Conf. 3D Dig. Imag. Modelling*, pp. 191-200.

[8] R. T. Whitaker, J. Gregor, and P. T. Chen. Indoor scene reconstruction from sets of noisy range images. *Proc. 3DIM'99*, pp. 348-357.

[9] J. V. Wyngaerd, et al. Invariant-based registration of surface patches. *Proc. 1999 IEEE ICCV*, 301-306.

[10] Z. Zhang. Iterative point matching for registration of free-form curves. *Technical report*, no. 1658, INRIA, May 1992.